Title
Numerical studies of CO2 and brine leakage into a shallow aquifer through an open wellbore

Journal
Hydrogeology Journal, 26(2)

ISSN
1431-2174

Authors
Wang, Jingrui
Hu, Litang
Pan, Lehua
et al.

Publication Date
2018-03-01

DOI
10.1007/s10040-017-1685-y

Peer reviewed

Numerical studies of CO_2 and brine leakage into a shallow aquifer through an open wellbore

Jingrui Wang[1], Litang Hu[1], Lehua Pan[2], Keni Zhang[2]

1 College of Water Sciences, Engineering Research Center of Groundwater Pollution Control and Remediation of Ministry of Education, Beijing Normal University, Beijing, China

2 Energy Geosciences Division, Lawrence Berkeley National Laboratory, Berkeley, CA, USA

Litang Hu litanghu@bnu.edu.cn; Jingrui Wang wangjr@mail.bnu.edu.cn; Lehua Pan lpan@lbl.gov; Keni Zhang kzhang@lbl.gov

Abstract

Industrial-scale geological storage of CO_2 in saline aquifers may cause CO_2 and brine leakage from abandoned wells into shallow fresh aquifers. This leakage problem involves the flow dynamics in both the wellbore and the storage reservoir. T2Well/ECO2N, a coupled wellbore-reservoir flow simulator, was used to analyze CO_2 and brine leakage under different conditions with a hypothetical simulation model in water-CO_2-brine systems. Parametric studies on CO_2 and brine leakage, including the salinity, excess pore pressure (EPP) and initially dissolved CO_2 mass fraction, are conducted to understand the mechanism of CO_2 migration. The results show that brine leakage rates increase proportionally with EPP and inversely with the salinity when EPP varies from 0.5 to 1.5 MPa; however, there is no CO_2 leakage into the shallow freshwater aquifer if EPP is less than 0.5 MPa. The dissolved CO_2 mass fraction shows an important influence on the CO_2 plume, as part of the dissolved CO_2 becomes a free phase. Scenario simulation shows that the gas lifting effect will significantly increase the brine leakage rate into the shallow freshwater aquifer under the scenario of 3.89% dissolved CO_2 mass fraction. The equivalent porous media (EPM) approach used to model the wellbore flow has been evaluated and results show that the EPM approach could either under- or over-estimate brine leakage rates under most scenarios. The discrepancies become more significant if a free CO_2 phase evolves. Therefore, a model that can correctly describe the complex flow dynamics in the wellbore is necessary for investigating the leakage problems.

Keywords: CO_2 leakage. Multiphase flow. Numerical modeling. Drift flux model. Equivalent porous media approach

Introduction

Greenhouse gas emissions caused by human activities, such as the burning of fossil fuels, are believed to be responsible for the increase in atmospheric temperature since the industrial revolution. The geological storage of CO_2 in saline aquifers has been recognized as one of the most significant potential ways to mitigate this problem (Bachu 2000; Yamamoto et al. 2009; Zhu et

al. 2015; Xie et al. 2015); however, the leakage of CO_2 and brine from deep storage reservoirs into shallow aquifers is a major risk for CO_2 geological storage projects (Pawar et al. 2009; Birkholzer et al. 2011; Esposito and Benson 2012; Namhata et al. 2017). The invasion of freshwater aquifers by leaked CO_2 and brine may pose great risks to human health and the ecological environment. Various studies have demonstrated that the leaking CO_2 and brine can detrimentally affect water quality in overlying potable aquifers, possibly to the extent that the water ceases to be potable (Zheng et al. 2009; Apps et al. 2010). The impacts of elevated CO_2 concentration in the shallow subsurface could also include lethal effects on plants and subsoil animals (Abanades et al. 2005). Open wells, such as abandoned wells, occur widely in mature sedimentary basins and can serve as conduits for CO_2 and brine leakage, which will significantly alter fluid flow and heat transfer in the vicinity of the open well (Hu et al. 2011; Zhang and Bachu 2011). For the safety of CO_2 geological storage, it is essential to reveal the mechanism of CO_2 and brine migration through open wells.

The leakage of CO_2 and brine into a shallow aquifer from a deep CO_2 storage reservoir through an open wellbore involves complex flow dynamics in both the formations and the wellbore. A number of modeling studies have depicted the wellbore as a porous medium and Darcy's Law has been used to simulate the brine or CO_2 leakage rate along the wellbore (Nordbotten et al. 2009; Humez et al. 2011; Tao and Bryant 2014; Tao et al. 2014; Harp et al. 2016; Yu et al. 2016; Ford et al. 2017)—for instance, Birkholzer et al. (2011) used the equivalent permeability value of 10^{-12} m^2 for the geological formation in which CO_2 injection took place, and a relatively large value of 10^{-8} m^2 for the wellbore. Hu et al. (2012) evaluated the equivalent permeability of the wellbore by fitting the brine leakage rate from the equivalent porous media (EPM) approach with that from T2Well/ECO2N, and considered that the value can reach up to 10^{-6} m^2. In the Tao and Bryant (2014) study, the equivalent permeability of about 300 wellbores was estimated in order to model the CO_2 leakage rate, and the expected values along most of the leaky wellbores were in the range of 10^{-11} and 10^{-8} m^2. CO_2 leakage along preferential pathways (such as fractures, microannulus, gas channels) in the steel/cement/earth system caused by sustained casing pressure has also been studied, and the results showed that the effective permeability of the leakage path is in the range of microdarcies to hundreds of microdarcies (Tao et al. 2014). Bigi et al. (2013) developed a numerical model to simulate CO_2 leakage through the fractured rock outcrop, and the equation for velocity in the fracture follows a modified form of Darcy's Law, where the coefficients take into account the relatively small resistance to flow along the fractures. By this token, the equivalent permeability is not a certain value for different problems and Darcy's Law, i.e., the equivalent porous media (EPM) approach, is inaccurate in describing wellbore flow, especially when turbulent flow or phase changes are involved. Indeed, while the flow in the formations can be properly described by Darcy's Law in

general, the flow in the wellbore is more complicated than the linear relationship between the hydraulic gradient and the flow rate as described by Darcy's Law. The determination of the flow velocity in a wellbore involves solving the appropriate momentum conservation equations (Pan et al. 2011c).

Analytical (Nordbotten et al. 2004, 2009) and semi-analytical methods (Nordbotten et al. 2005; Pan et al. 2011a; Réveillère 2013) are usually used to forecast the flux of brine or CO_2 along the wellbore quantitatively. Numerical models are more accurate and computationally demanding when complicated hydrogeological and geological factors are included (Tao et al. 2011; Harp et al. 2016). What is more, very limited studies consider multiphase (e.g. liquid and gas) and multi-component flows in both the wellbore and in the porous media reservoir. Analytical methods provide a tool to analyze leakage problems in a single liquid phase (Nordbotten et al. 2004). Réveillère (2013) presented a semi-analytical solution of brine leakage along the wellbore by taking account of the effect of the density difference between lifting and lifted brines during both upward and downward flow. Tao et al. (2011) estimated the single CO_2 phase flow rate along a defect by using the established model; however, only the single-phase flow was considered in these solutions, which is not applicable for problems with multi-phase flow, such as the exsolution of CO_2 from the aqueous phase and transition of the fluid flow in the wellbore from single phase flow to two-phase flow. The process of two-phase flow in the wellbore is very different to that of the single phase, because the density of gas is smaller than that of the brine. To evaluate the CO_2 and brine leakage rate along the wellbore, a model of multi-phase fluid flows along the leakage pathway is required to mimic the process.

This study is an extension of the work by Hu et al. (2012), who only considered the brine leakage to a shallow freshwater aquifer through an open wellbore in the water-brine system. The objective of this paper is to investigate the influences of both salinity and dissolved CO_2 on the cross-formation leakage through the wellbore in the water-CO_2-brine system using the T2Well/ECO2N simulator. Parametric studies and sensitivity analysis on CO_2 and brine leakage will be conducted, which include excess pore pressure (EPP), salinity and CO_2 mass fraction. It is assumed that all of these three parameters are independent of each other. The CO_2 and brine leakage from the reservoir to the fresh aquifer in different scenarios will be discussed in detail. The results from the coupled wellbore-reservoir simulator will be compared with the results from the EPM model to determine the applicability of the EPM method.

Model setup

Simulator

The simulator used in this work is T2Well/ECO2N, a fully coupled wellbore-reservoir simulator of a water-CO_2-brine system (Pan et al. 2011b; Pan and

Oldenburg 2014). This simulator models the reservoir-wellbore system as two related sub-domains with different physical laws. In the reservoir sub-domain, the phase velocity is obtained by directly using a multiphase version of Darcy's Law. However, in the wellbore domain, the phase velocity is obtained by solving a one-dimensional momentum equation for a fluid mixture, where the drift-flux model is used to model the interfacial interactions between the gas and liquid phases (Pan et al. 2011a). Simultaneously solving the coupled wellbore-reservoir flow equations is difficult work. The integrated finite difference scheme in TOUGH2 software is used to discretize the conservation equations in space for both the wellbore and the reservoir. Time is discretized as a first-order, fully implicit finite difference, apart from the special treatment of the momentum equation in the wellbore. A mixed implicit-explicit scheme is applied to solve the momentum equation, because the definition of velocity in the wellbore is different from that in the reservoir. In this way, the equations for the wellbore cells can be seamlessly fitted into the TOUGH2 framework with the same iteration and time-stepping methods (Pan and Oldenburg 2014). The flow terms at the interface between the perforated wellbore sections and the surrounding porous media are calculated using Darcy's Law, while the nodal distance to the interface on the wellbore side is set to zero to eliminate the effect of resistance to flow inside the wellbore. The heat exchanges between the wellbore and the surrounding formation are calculated as the normal heat flow terms in the standard TOUGH2 if the surrounding formation is explicitly in the numerical grid. It can also be calculated semi-analytically if no grid blocks of surrounding formation exist. The wellbore model can be turned off easily by modifying the input file, and the standard TOUGH2/ECO2N simulator will be used instead; and thus, the equivalent porous media (EPM) approach has been adopted. For the EPM approach, all the parameters are the same as those for the coupled wellbore-reservoir model, and the wellbore is represented as a porous medium with a very high permeability and a porosity of 1. The T2Well/ECO2N simulator has been integrated into the Well Leakage Analysis Tool (WLAT) to analyze the risk of CO_2 leakage along the wellbore (Huerta and Vasylkivska 2015). The details of the methodology and the validation of the T2Well module can be found in Pan et al. 2011b and Pan and Oldenburg 2014, and will not be repeated here.

Conceptual model

When CO_2 is injected into an aquifer, the region of significant pressure increase extends much further in the lateral direction than the limited extent of the CO_2 plume, and the dissolved CO_2 plume extends to a limit that falls between them (Birkholzer et al. 2009). This study mainly focuses on the region between the plume front of the dissolved CO_2 and the plume front of free CO_2. A hypothetical two-aquifer and one-well system is established. The model consists of a shallow freshwater aquifer and a deep CO_2 storage reservoir, separated by poorly permeable mudstone but connected by an open well that penetrates the mudstone (Fig. 1). The freshwater aquifer

extends to approximately 700 m below the ground surface, while the CO_2 storage reservoir lies between 2,200 and 2,300 m deep. The thickness of the mudstone, which serves as the cap rock of the CO_2 geological storage, is 1,500 m. The hypothetical passive (existing, other than the injection well) wellbore with a diameter of 0.12 m passes through both aquifers (fully perforated) and the mudstone formation (perfectly cased). This paper is mainly focused on the influences of CO_2 leakage on the shallow groundwater system, and so the wellbore is assumed to be sealed at the surface (wellhead). The well casing in contact with the mudstone formation is assumed to allow only heat exchange (i.e., no mass flux) between the wellbore and the surrounding mudstone. The non-isothermal flow condition and the contact with the mudstone formation concerned here aim at eliminating the effect of temperature on the results. A radially symmetric mesh is developed with considerable grid refinement near the well and near the formation interfaces. Vertically, three geologic properties were assigned to 53 grid layers, and fine grid spacings (nodal spacing from 1.0 to 74 m) were used for the vicinity of the formation interfaces. The area within a 100-m range from the wellbore was radially remeshed with nodal spacing from 0.12 to 14 m (see Fig. 1). The radius of the model domain is 2,000 m. Hereinafter, *Z* and *R* represent the depth below the surface and the radial distance from the well, respectively.

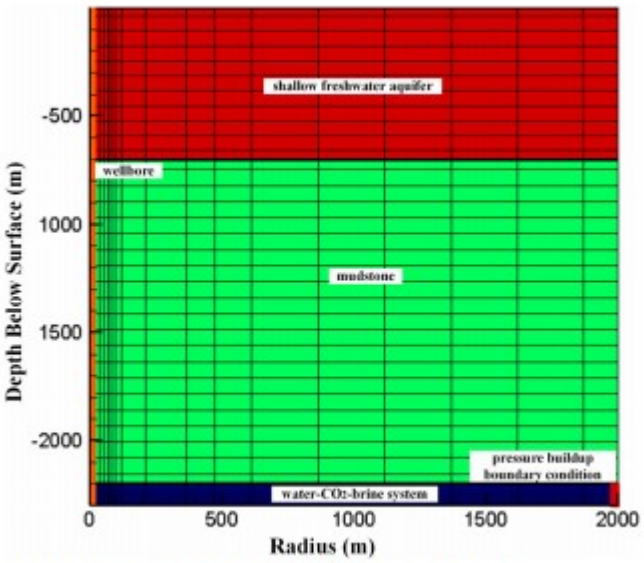

Fig. 1 Radially symmetric model for dynamic simulations

Table 1 summarizes the system configurations and parameters used in the simulations. Most of the hydrogeological parameters that drive the models are set based on the first CO_2 capture and sequestration project in northeastern part of the Ordos basin, China (Xie et al. 2015; Zhang et al. 2016). A seismic survey conducted in 2010 revealed the structural characteristics of the underground formations. Four possible combinations of reservoir (the Liujiagou Formation, the Shiqianfeng Formation, the Shihezi

Formation and the Shanxi Formation) and seal (Heshanggou Formation) in the Triassic and Permian systems were recommended for CO_2 sequestration. Rough estimates indicate that the storage capacity of the Ordos basin for CO_2 is over 10 billion tonnes (Zhang et al. 2016). Liu et al. (2015) indicated that the Liujiagou Formation, with permeability ranging from 10^{-13} to 10^{-11} m^2 and porosity ranging from 0.01 to 0.3, had the highest mineral trapping capacity. At the early stage, most of the numerical simulations were carried out without considering the heterogeneity of the injection formations. Recently, Li et al. (2016) indicated that the permeability heterogeneity might have a strong influence in the reservoir performance. In this study, all formations are simplified and assumed to be saturated with water and horizontally heterogeneity. The initial pressure and salinity field of the model are assumed to be under hydrostatic equilibrium in the system, with a linear distribution of salinity along the depth. The geothermal gradient is set to 27 °C/km. The initial temperature field is assumed to vary linearly with a geothermal gradient from 8 °C at the top of the model to 77 °C at the bottom. The permeability of the reservoir and seal formation is set to 10^{-12} m^2 and 10^{-15} m^2, respectively. The relative permeability is calculated by the van Genuchten-Mualeum model, and capillary pressure is calculated using the van Genuchten function (van Genuchten 1980; Mualem 1976). Irreducible water saturation, residual CO_2 saturation, liquid saturated saturation and gas saturated saturation are set to 0.15, 0.18, 1.0 and 0.999, respectively. The parameter m in van Genuchten's notation is set to 0.4 by convention and the capillary entry pressure is set to 3.58 MPa. The thermal conductivity of all the formations is set to 2.51 W/(mK). The pore compressibility is not considered in this simple model. The top layer of the model is the atmosphere, where the pressure is atmospheric pressure, while the bottom layer of the domain is assumed to be a closed boundary for fluid and dissolved salt. The top and bottom of the wellbore are all assumed to be closed. The excess pore pressure (EPP) is imposed at the outer boundary (i.e., at R = 2,000 m) of the storage reservoir, and the outer boundary is treated as a Dirichlet boundary condition by setting a big volume (e.g. 10^{50} m^3) to the grid (Fig. 1). It is assumed that the EPP of the outer boundary is constant within the simulation period, and dissolved CO_2 exists in the storage reservoir. Non-isothermal processes are simulated, including the fluid and heat flow between the wellbore and the surrounding formation (both sand and mudstone), as well as those within the formations. Based on the pervious study by Hu et al. (2012), the flow in the model will reach equilibrium state after 10 days and so the simulation period of all the models is set as 10 days in this study.

Table 1 Properties of simulation cases

Parameter		Unit	Value	Comment
All rock units				
	Porosity	–	0.3	–
	Thermal conductivity	W/(mK)	2.51	–
	Heat capacity	J/(kgK)	1000	–
	Pore compressibility	Pa^{-1}	0	Pore compressibility is not considered in this simple model
	Permeability of the CO_2 storage reservoir	m^2	10^{-12}	Isotropic
	Permeability of the mudstone formation	m^2	10^{-18}	Isotropic
	Permeability of the shallow aquifer	m^2	10^{-12}	Isotropic
Well properties				
	Well radius	m	0.12	–
	Porosity	–	1.0	–
	Maximum C_0 (the profile parameter)	–	1.2	–
	Roughness	–	0.000046	–
Relative permeability and capillary pressure related parameters				
	m parameter in van Genuchten's notation	–	0.40	–
	Irreducible water saturation	–	0.15	–
	Maximum water saturation	–	1.0	–
	Residual CO_2 saturation	–	0.18	–
	Capillary entry pressure	KPa	3.58	–

The dissolved CO_2 mass fractions in the reservoir are set as 0.10, 0.50, 1.00, 3.00 and 3.89%. The combination scenarios are listed in Table 2, including five dissolved CO_2 mass fractions, four EPP variations (0.1, 0.5, 1.0 and 1.5 MPa), and four salinity variations (2.5, 5.0, 7.50 and 15.00%), for a total of 80 scenarios.

Table 2 Scenarios for parametric studies

Dissolved CO_2 mass fraction in reservoir (%)	Salinity (%)	Excess pore pressure, EPP (MPa)
0.10	–	–
0.50	2.50	0.1
1.00	5.00	0.5
3.00	7.50	1.0
3.89	15.00	1.5

Results and analysis

Brine leakage rate under different salinity and EPP scenarios

EPP will push the brine with dissolved CO_2 upward along the open well. For low EPP scenarios (0.1 MPa) with a fixed dissolved CO_2 mass fraction (1.00%), the brine flow rate from the reservoir to the shallow aquifer arrives at the peak within 1 day, then decreases and finally reaches zero (Fig. 2a). The brine from the reservoir will replace part of the water stored in the wellbore (Fig. 3a), and the gravity of fluid in the wellbore will increase with its density. Part of the brine initially in the wellbore will enter the freshwater

aquifer. Then the upward movement driven by relatively small EPP (0.1 MPa) is balanced by the increased gravity and a new equilibrium will be obtained; however, little (2.50% salinity scenario) or no brine (5.00 and 7.50% salinity scenarios) from the reservoir will enter the freshwater aquifer, which can be explained by the appearance of brine in the fresh aquifer, but no dissolved CO_2 is present. Because only the brine from the reservoir has dissolved CO_2, the dissolved CO_2 can be regarded as a tracer. When EPP is 0.5, 1.0 and 1.5 MPa, the brine flow rate to the shallow aquifer increases rapidly and becomes almost constant after 3 days. The brine flow rates after 10 days are 14.0–19.6, 24.8–28.5, and 32.7–35.5 kg/s for 0.5, 1.0, and 1.5 MPa EPP, respectively. It can be observed that the brine leakage rates after 10 days increase almost proportionally with the EPP when a sustained flow exists, while the brine leakage rates increase inversely with the salinity because of the gravitational effect.

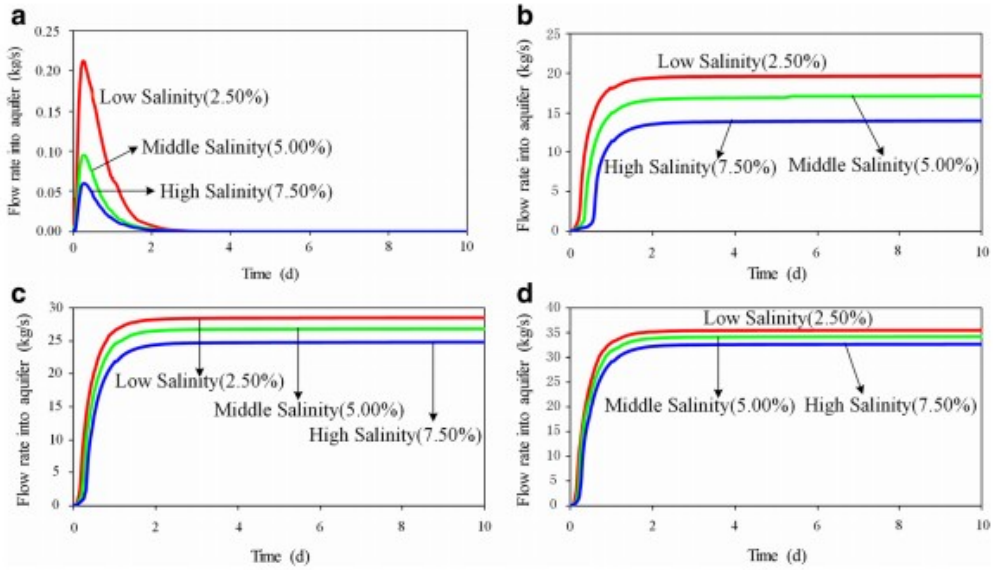

Fig. 2 Change in rate of brine flow into the shallow freshwater aquifer with time under different salinities, a fixed dissolved CO_2 mass fraction (1.00%) and different EPP: **a** 0.1 MPa; **b** 0.5 MPa; **c** 1.0 MPa; **d** 1.5 MPa

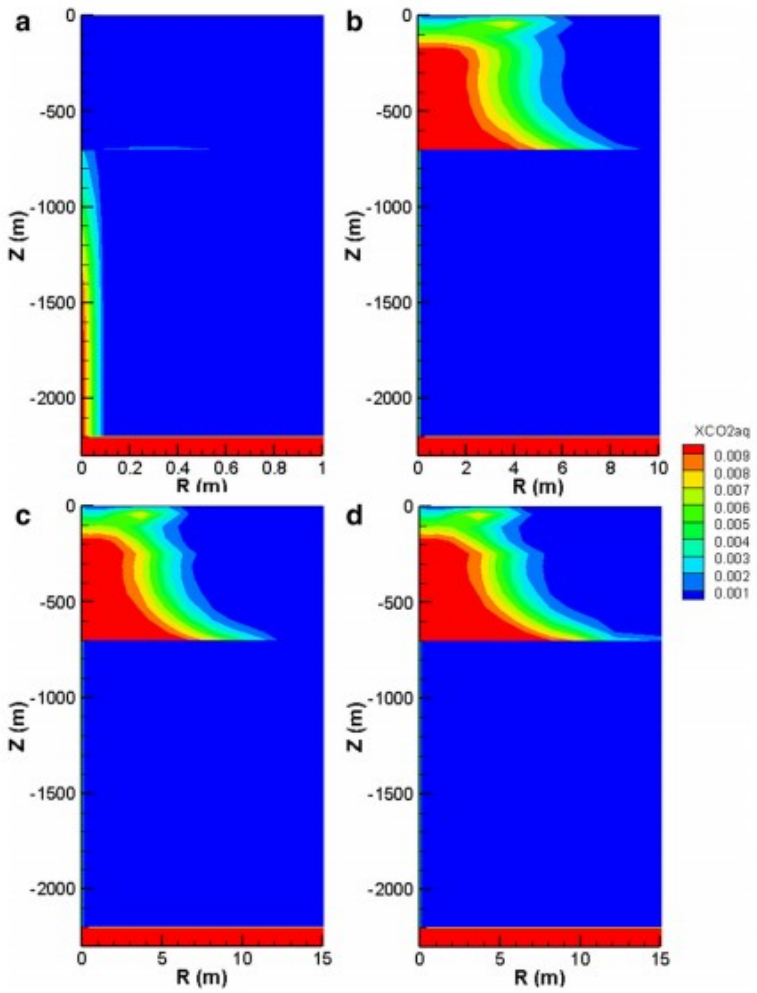

Fig. 3 Colormap of dissolved CO_2 mass fraction in aqueous phase along the radial distance after 10 days with 2.50% salinity, fixed dissolved CO_2 mass fraction (1.00%) and different EPP values: **a** 0.1 MPa; **b** 0.5 MPa; **c** 1.0 MPa; **d** 1.5 MPa

CO_2 leakage under different salinity and EPP scenarios

The scenarios of 2.50% salinity under the EPP of 0.1, 0.5, 1.0 and 1.5 MPa with a fixed CO_2 mass fraction (1.00%) were chosen to analyze CO_2 leakage along the open well. As shown in Fig. 3, for the low EPP (0.1 MPa), the driving force induced by the EPP is balanced by the gravity of saline in the wellbore after 10 days, and thus there is little CO_2 leakage to the fresh aquifer; however, for the other scenarios with the EPPs of 0.5, 1.0 and 1.5 MPa, there is significant CO_2 leakage, and the shapes of the dissolved CO_2 plume are similar. The movement of CO_2 in the shallow freshwater aquifer depends on many factors, such as the dissolution/exsolution of CO_2 with water, the capillary forces and the gravity forces. The distance that dissolved CO_2 migrates away from the wellbore increases with EPP. The distances that dissolved CO_2 migrates along the interface between the fresh aquifer and mudstone ($Z = -700$ m) are approximately 10 and 20 m after 10 days for the 0.5 and 1.5 MPa scenarios (Fig. 4a,b), respectively.

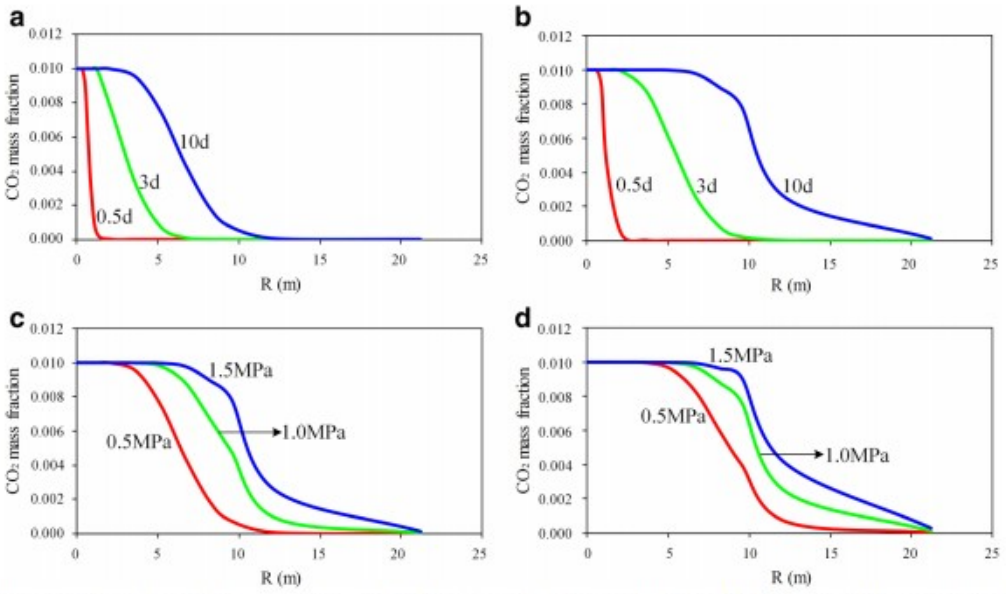

Fig. 4 Change in CO_2 mass fraction in aqueous phase, with radial distance at $Z = -700$ m and with fixed 1.00% dissolved CO_2 mass fraction: **a** EPP of 0.5 MPa and salinity of 2.50%; **b** EPP of 1.5 MPa and salinity of 2.50%; **c** salinity of 2.50% after 10 days; **d** salinity of 7.50% after 10 days

Figure 4c,d shows the change in the dissolved CO_2 mass fraction with radial distance at the interface between the mudstone and shallow freshwater aquifer under different salinity and EPP scenarios after ten days. Under the same salinity scenarios, the longest distance that CO_2 migrates depends on the value of the EPP, and the fixed 2.50% salinity scenarios are also visually shown in Fig. 3b,d. However, the fluid with higher salinity will impede the upward migration of the fluid, and thus, the front of the fluid with higher salinity (7.50% salinity scenario) is more prone to migrate radially along the interface between the mudstone and shallow freshwater aquifer than that of the fluid with lower salinity (2.50% salinity scenario). As shown in Fig. 4c,d, the distance that the CO_2 migrates along the interface between the mudstone and shallow freshwater aquifer increases with the salinity, though the brine leakage rate of the 7.50% salinity scenario (24.8 kg/s) is smaller than that of the 2.50% salinity scenario (28.5 kg/s; Fig. 2)—for example, under the scenarios of EPP with 1.0 MPa, the distances are approximately 15 and 21 m for 2.50 and 7.50% salinity, respectively, due mainly to the effect of the salinity on the upward migration of the brine and CO_2.

It should be noted that dissolved CO_2 will experience phase transitions when it moves towards the top of the fresh aquifer along the open well.
Figure 5 shows the changes in free CO_2 phase saturation with radial distance along the top of the fresh aquifer under different salinity and EPP scenarios. For scenarios with the same dissolved CO_2 mass fraction, EPP and salinity are the dominant factors influencing the migration of gaseous CO_2. The distances that the free CO_2 phase migrates are approximately 5 and 4 m for 2.50 and 5.00% salinity (the result of the 5.00% salinity scenario is also visually shown in Fig. 7a), respectively, with the same EPP of 0.5 MPa (Fig. 5a). The farthest distance that CO_2 moves is approximately 5 m for the EPP scenarios of

1.5 MPa. High EPP may lead more fluid leak to the fresh aquifer, and thus, more CO_2 transit from the dissolved state to the free gas state. When EPP is relatively low (e.g., 0.5 MPa), the salinity will significantly affect the upward movement of CO_2, so there is less CO_2 phase transition when the salinity increases from 2.50 to 5.00%. In contrast, when the EPP is relatively high (e.g., 1.5 MPa), the salinity has less effect on the movement of the free CO_2 phase, and the distance that free CO_2 phase migrates along the top of the fresh aquifer is very similar for scenarios with different salinity (Fig. 5b).

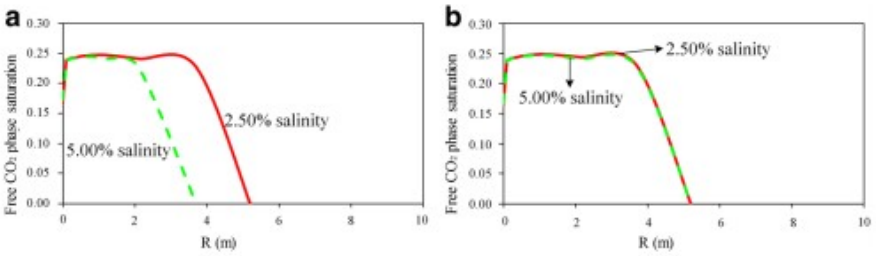

Fig. 5 Changes in gas (CO_2-rich) phase saturation with radial distance under different salinity and EPP scenarios at the top of the fresh aquifer: **a** EPP of 0.5 MPa; **b** EPP of 1.5 MPa

Influences of the dissolved CO_2 mass fraction on CO_2 leakage

To understand how the dissolved CO_2 mass fraction of the reservoir fluid affects the shape of the dissolved CO_2 plume, four scenarios were examined, where EPP and salinity were set to 0.5 MPa and 5.00%, respectively, and the dissolved CO_2 mass fraction was set as 0.10, 0.50, 1.00 and 3.00%. The CO_2 plume migration is influenced by both the dissolved CO_2 mass fraction and salinity. When the dissolved CO_2 mass fraction is relatively low (0.10 and 0.50%), the dissolved CO_2 plume (Fig. 6a,b) is driven by the pressure gradient and expands horizontally, but tends to remain close to the bottom of the aquifer because brine is heavier than fresh water. The horizontal distance that the CO_2 migrates increase with the salinity, which is shown in Fig. 4c,d. Besides, no free CO_2 phase appears in the two scenarios. Therefore, the salinity plays a dominant role in the migration of the dissolved CO_2 plume in the two scenarios (Fig. 6e,f). Noticeably, the maximum height of brine migration for the 0.10% dissolved CO_2 mass fraction is a little bit higher than that for the 0.50% dissolved CO_2 mass fraction, which is caused by the fact that the solution of CO_2 into water increases the density of the saline water (Fig. 10). However, when the dissolved CO_2 mass fraction in the reservoir is increased above 1.00%, a free CO_2 phase is evolved, and movement of the free CO_2 phase has certain influences on the shape of the dissolved CO_2 plume (Fig. 6c,d).

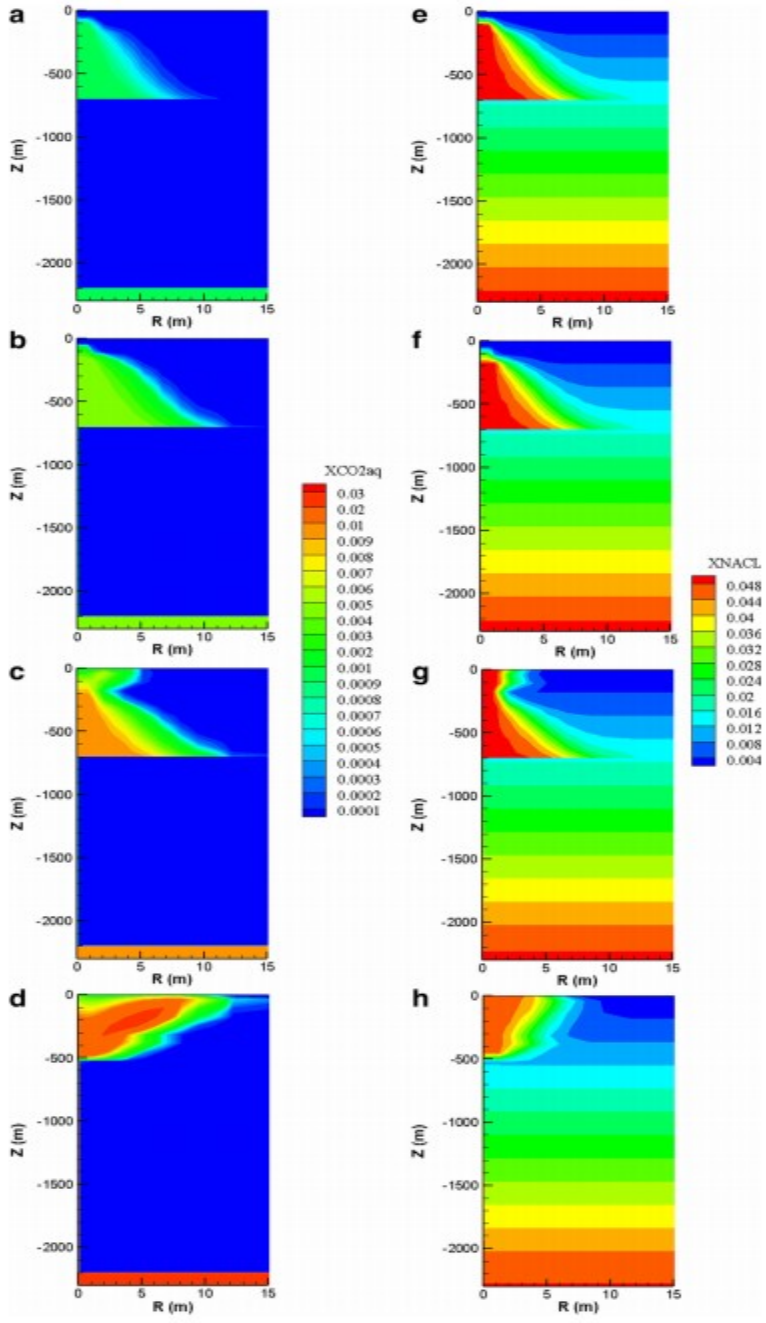

Fig. 6 Colormap of the dissolved CO_2 mass fraction and salinity (NaCl) along the radial distance after 10 days under the EPP of 0.5 MPa, 5.00% salinity and different dissolved CO_2 mass fractions in the aqueous phase: **a** 0.10%, dissolved CO_2 mass fraction; **b** 0.50%, dissolved CO_2 mass fraction; **c** 1.00%, dissolved CO_2 mass fraction; **d** 3.00%, dissolved CO_2 mass fraction; **e** 0.10%, salinity; **f** 0.50%, salinity; **g** 1.00%, salinity; **h** 3.00%, salinity

Once brine leakage into the wellbore is induced by EPP, it will migrate upwards along the well and move rapidly into the wellhead. As the brine moves upward along the wellbore, part of the dissolved CO_2 becomes a free phase, because the pressure and temperature change greatly (Fig. 7; Steel

et al. 2016). Because of its low density, the free CO_2 phase will migrate upward rapidly and then move horizontally when it is close to the wellhead (Fig. 7). The appearance of the free CO_2 phase significantly affects the migration of the brine. In this situation, part of the brine will migrate upwards with the free CO_2 phase. The free CO_2 phase exerts a great influence on the dissolved CO_2 plume after 10 days; however, a large part of the CO_2 plume still tends to be close to the bottom of the aquifer (Fig. 6g).

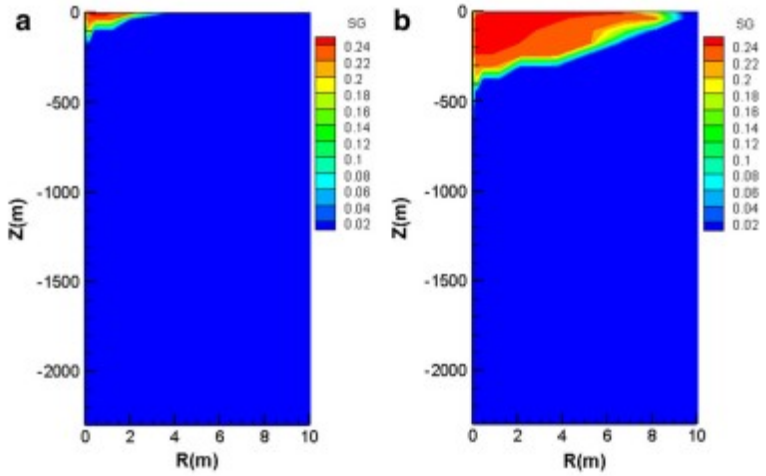

Fig. 7 Colormap of the saturation of gas phase (SG) along the radial distance after 10 days under the EPP of 0.5 MPa, 5.00% salinity and different dissolved CO_2 mass fractions: **a** 1.00%; **b** 3.00%

Compared with the 1.00% dissolved CO_2 mass fraction scenario, there is a greater appearance of the free CO_2 phase for the 3.00% scenario (Fig. 7a,b). The free CO_2 phase begins to appear when it passes through the wellbore depth of 100 m for the 1.00% dissolved CO_2 mass fraction scenario, whereas the value is approximately 500 m for the 3.00% dissolved CO_2 mass fraction scenario. As a consequence, the upward migration of the free CO_2 phase dominants the migration of not only the dissolved CO_2 plume, but also the brine plume, and both of them migrate in a upward tendency (Fig. 6c–f).

The scenario under the EPP of 0.5 MPa with 3.00% dissolved CO_2 mass fraction and 5.00% salinity was used to analyze the evolution of the free CO_2 phase in the wellbore. The pressure, temperature and mass fraction of dissolved CO_2 in brine are the main factors that affect the exsolution of CO_2 from brine. The time period from 0.511 to 0.533 d may be a critical time for this scenario, where the dissolved CO_2 evolves into the gas phase, and thus the times of 0.511, 0.533 and 10 d were selected to show time profiles in Fig. 8b. When the simulation time is 0.511 d, the mass fraction of dissolved CO_2 at the depth of approximately 590 m below the wellhead reaches 1.30% (Fig. 8a). Under the relatively low pressure, the dissolved CO_2 evolves into the gas phase (Fig. 8b). After that point, with the continuous migration of fluid from the reservoir to the wellbore, a substantial free CO_2 phase appears. After approximately 3 days of simulation, the flow becomes almost steady state. The mass fraction of the dissolved CO_2 and saturation of the free CO_2 phase in the wellbore are nearly constant, which is very close to the state at the 10th day.

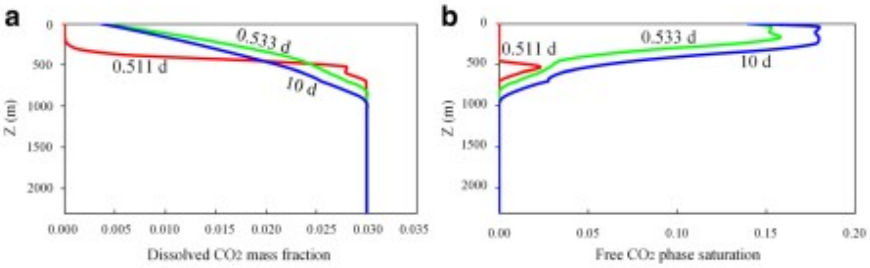

Fig. 8 Mass fraction of **a** dissolved CO_2 and **b** free CO_2 phase saturation in the wellbore with EPP of 0.5 MPa, 3.00% dissolved CO_2 mass fraction and 5.00% salinity

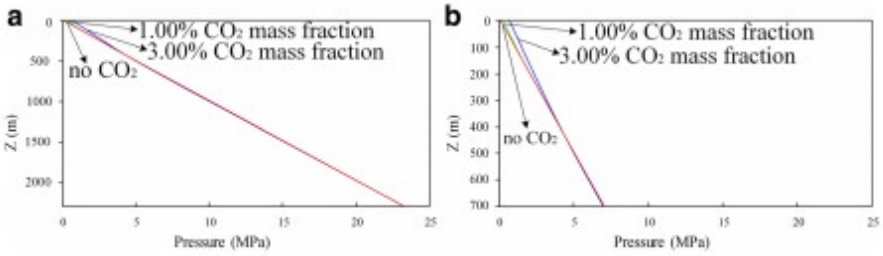

Fig. 9 Pressure distribution along the wellbore after 10 days with the EPP of 0.5 MPa and salinity of 5.00%: **a** at depth between 0 and 2,300 m, **b** at depth between 0 and 700 m

Influences of the CO_2 mass fraction on the pressure field

To determine the influence of the CO_2 mass fraction on the pressure field, the following three scenarios with fixed salinity of 5.00% and fixed EPP of 0.50 MPa were considered: (1) no CO_2; (2) 1.00% CO_2 mass fraction and (3) 3.00% CO_2 mass fraction. Figure 9 demonstrates the pressure distribution along the depth in the wellbore. The pressure distributions in the wellbore below 700 m are similar for all three scenarios except for the 3.00% case which has slightly lower pressure approaching the depth of 700 m (the outlet of non-perforated section of the wellbore); however, in the upper portion of the wellbore, the pressure drop starts to slow down due to occurrence of the gas phase. This is because the gravity force needed to be overcome is significantly reduced due to the lower density of the gas phase. As shown in Fig. 10, the average density of fluid (brine and gas) changes significantly as it approaches the top of the wellbore. Because there is more CO_2 in the 3.00% case, which resulted in a larger two-phase region than for the 1.00% case, the lower-density region is larger in the 3.00% case than in the 1.00% case (Fig. 10). As a result, the deviation of pressure in the 3.00% case from that in the no-CO_2 case is also larger than that in the 1.00% case (Fig. 9).

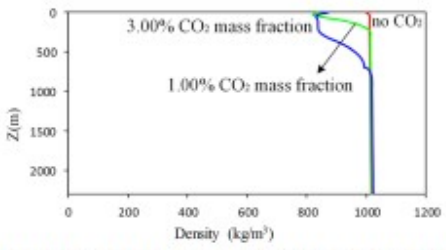

Fig. 10 Distribution of mixture density along the wellbore after 10 days for three initial dissolved CO_2 mass fraction scenarios, with the EPP of 0.5 MPa and salinity of 5.00%

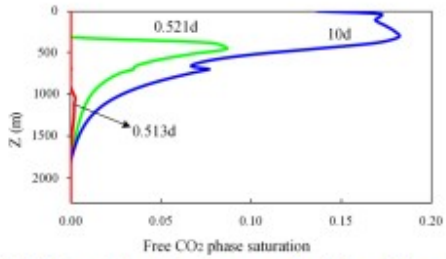

Fig. 11 Evolution of free CO_2 phase saturation in the wellbore with the EPP of 0.5 MPa, 3.89% dissolved CO_2 mass fraction and 5.00% salinity

Discussion

Appearance of the free CO_2 phase and its effect on brine leakage

To investigate how the appearance of the free CO_2 phase affects brine leakage, the case of an EPP of 0.5 MPa, 5.00% salinity, and 3.89% dissolved CO_2 mass fraction in the brine was simulated. The CO_2 mass fraction of 3.89% is the saturated concentration of CO_2 in 5.00% salinity brine at pressure 9.7 MPa and temperature 56.5 °C (Duan and Sun 2003; Duan et al. 2006), which corresponds to the pressure and temperature at about 1,000 m depth in the well. This depth is 300 m below the shallow aquifer and 1,200 m above the injection reservoir so that the two-phase behavior of the wellbore flow could be investigated. Figure 11 shows the profile of the gas (CO_2-rich) phase along the wellbore after three time periods. After 0.513 days, the gas phase first appears at the depth of approximately 1,040 m in the wellbore. The two-phase region quickly expands in the wellbore to a depth between 400 and 1,500 m at time 0.521 d. At the end of the simulation (10 days), large amounts of free CO_2 phase are present in the wellbore (Fig. 11).

Figure 12a shows the brine leakage rates at the depth of 700 m (entering the shallow aquifer) up to 10 days for four cases: 0.00, 1.00, 3.00, and 3.89% dissolved CO_2 mass fraction in the reservoir under the same conditions of EPP 0.5 MPa and 5.00% salinity. Because dissolution of CO_2 will increase the density of the brine (Fig. 10), the leakage rate at early time decreases with the saturation of dissolved CO_2 (Fig. 12a); however, after the leaking brine reaches the shallow depth, the low pressure causes effervescence of CO_2 from the brine which changes the trend—for example, the brine leakage rates for these four scenarios after 10 days become 17.8, 17.1, 17.7 and 21.0 kg/s, respectively (Fig. 12a). This trend can be explained by the total hydraulic gradient ($dP/dz - \rho_m g$) shown in Fig. 13a, where P is the pressure, z is the depth below surface, ρmρm is the mixture density and g is the gravitational acceleration. The total hydraulic gradient is the driving force that brings the fluid (considered as a mixture if there are two phases) upward in the wellbore. In general, the occurrence of gas phase significantly reduced the average density of the fluid, resulting in higher total hydraulic gradient; however, because the two-phase region in the 1.00% case is too small and limited within the downstream, which is a few hundred meters above the bottom of the shallow aquifer, the total hydraulic gradient below the depth of 700 m is significantly smaller than that in the 0.00% case because of heavier brine. As a result, the leakage rate (measured at the depth of 700 m) is smaller in the 1.00% case than that in the 0.00% case. In the cases with higher CO_2 concentration (3.00 and 3.89%), the two-phase region reaches below the depth of 700 m so that the average density of the fluid (gas and brine) is significantly lower than that in the no-CO_2 case even although the brine density is still higher. The resulting increase in the total hydraulic gradient is proportional to the mass fraction of CO_2 in the CO_2-brine mixture.

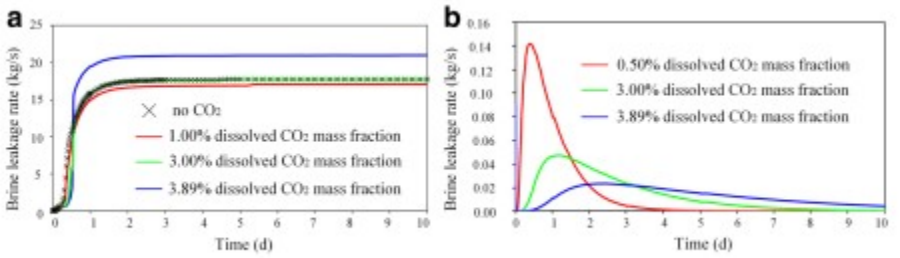

Fig. 12 Change in brine flow rate into the shallow aquifer with time for different initial dissolved CO_2 mass fractions and fixed EPP of 0.5 MPa: **a** with salinity of 5.00%; **b** with salinity of 15.00%

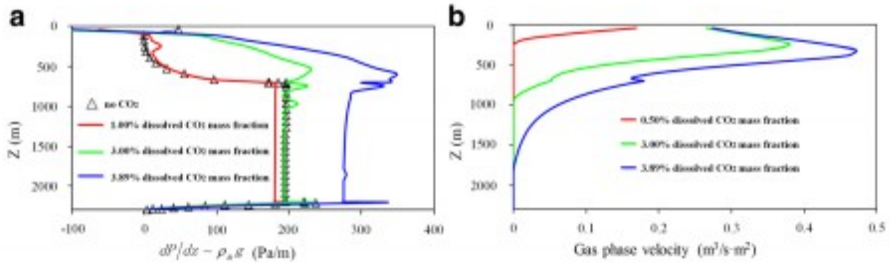

Fig. 13 Distribution of **a** the total hydraulic gradient, **b** gas phase velocity along the wellbore after 10 days for the scenarios with different initial dissolved CO_2 mass fractions

This gas-lifting phenomenon can also be seen with respect to the brine (liquid) phase flow. The fast upward flow of gas in the wellbore enhances the upward flow of liquid (brine). As shown in Fig. 13b, significant gas flow only takes place above the depth of 250 m in the 1.00% case, which does not help the brine flow at the depth of 700 m. As the CO_2 mass fraction increases to 3.00% or 3.89%, the gas flow starts to help the brine flow at increasing depth which resulted in much higher brine leakage rates at 700 m. Note that the maximum gas saturations in the wellbore below the depth of 700 m are only 0.0 (no-CO_2), 0.0 (1.00% CO_2), 2.68% (3.00% CO_2), and 7.63% (3.89% CO_2), respectively, which makes the gas-phase blockage (or interference) of brine flow not significant. The gas-phase leakage rate into the shallow freshwater aquifer after 10 days is 0.290 kg/s for the 3.89% case whereas it is only 0.084 kg/s for the 3.00% case.

Hu et al. (2012) found that a relatively higher salinity of the fluid can, to some extent, impede the saline leakage into the shallow fresh aquifer (for example, the scenario where the EPP and salinity are 0.5 MPa and 15.00%, respectively); here, it is called a “the self-limiting effect”. To investigate whether the self-limiting effect still exists when the dissolved CO_2 mass fraction increases, many scenarios were examined, including a combination of the dissolved CO_2 mass fractions of 0.50, 3.00 and 3.89%, the EPP of 0.5 MPa, and the salinity of 15.00%. The results show that for the three scenarios, the brine leakage rates increase at the beginning and then decline, and eventually drop to nearly zero (Fig. 12b). The peak value increases inversely with the dissolved CO_2 mass fraction, because the dissolution of CO_2 increases the density of the brine. With the exsolution of dissolved CO_2, the leakage rates will increase, and it also takes much more time for leakage rates to reach the peak for scenarios with 3.00% and 3.89% dissolved CO_2 mass fraction. So one can still find that the self-limiting

phenomenon exists when the dissolved CO_2 mass fraction increases (Fig. 12b). That is to say, the gas phase can contribute to the increase of brine leakage rate when its mass fraction is relatively high; however, it is not a decisive factor that affects whether the brine can leak into the shallow fresh aquifer. So, whether brine leakage occurs mainly depends on the mutual influences of the EPP and the gravity of the fluid. The influences of the initial CO_2 mass fraction may happen in the case of the exsolution of the dissolved CO_2. The exsolution/solution of CO_2 will slightly change the density of saline water; however, the influence is so small that it can be neglected when compared with the influences of EPP and the gravity of the fluid in this study.

Comparison of T2Well with the EPM method

The EPM method has been widely used to simulate wellbore flow (Birkholzer et al. 2011; Jung et al. 2013); however, the flow in the wellbore can be non-Darcian. Hu et al. (2012) found that equivalent permeability is an important parameter for the EPM approach and has important influences on the simulated leakage rate. Compared with T2Well/ECO2N, the EPM approach may over-estimate the leakage rate when the brine leakage rate is relatively high.

In this paper, the results from the EPM method and T2Well/ECO2N were also compared to test the applicability of EPM to the two-phase flow (CO_2-brine) condition. Previous researchers have demonstrated the large variance of wellbore permeability due to the non-linear wellbore flow. The equivalent permeability of 3.16×10^{-6} m^2, which is from Hu et al. (2012), is also adopted in this study. The cases of 1.00% dissolved CO_2 mass fraction and 3.00% dissolved CO_2 mass fraction with fixed 5.00% salinity were used for comparative analysis.

The simulation shows that the simulated colormaps of the dissolved CO_2 plume from T2Well are very different from the results of EPM (Figs. 6 and 14). The dissolved CO_2 plume from the EPM method is triangular, which is very similar to the results from the no-CO_2 cases (Fig. 14a,b), while the simulated plume using T2Well is irregular. The colormaps of the free CO_2 phase show that considerable dissolved CO_2 is changed to the gas phase (Fig. 7) for the T2Well method, while only a small amount of free CO_2 appears for the EPM approach (Fig. 14c,d). What is more, the migration pathway of gas is nearly the same as that of the brine (Fig. 14d), because the migration of gas is dependent on the pressure gradient for the EPM method; however, the simulation results from T2Well show that the free CO_2 phase greatly affects the migration of dissolved CO_2 through gas lifting effects and phase interference. Thus, the EPM method will be not be effective when free CO_2 phase evolution is involved, while T2Well can not only simulate the process with the phase change but also the effects of interaction of different phases, for example, the gas lifting effect.

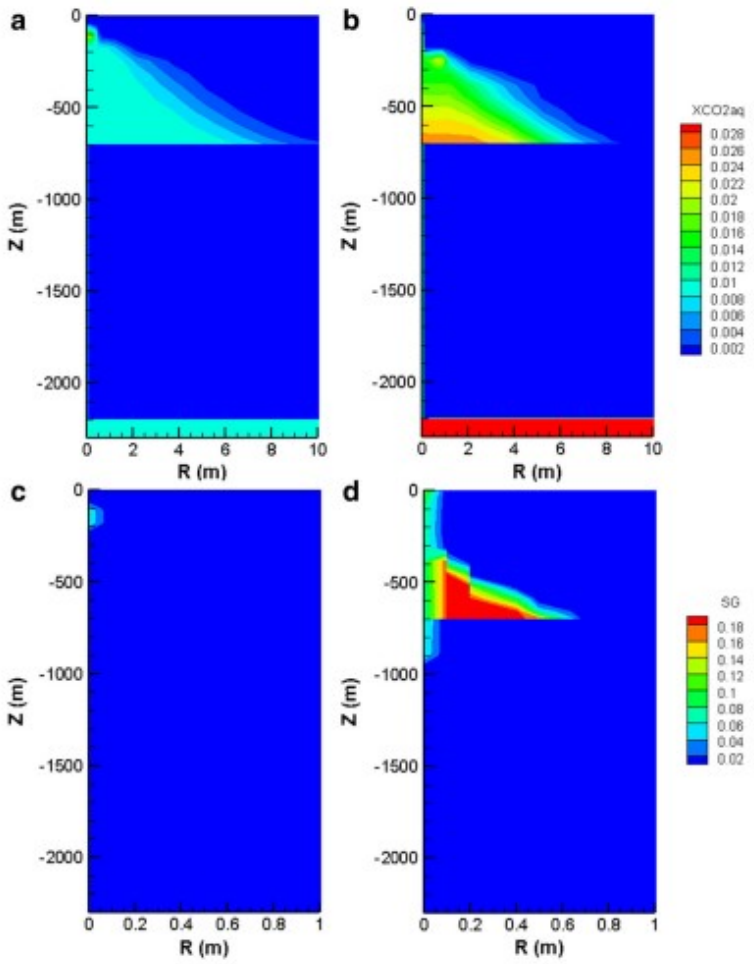

Fig. 14 Colormap of the dissolved CO_2 mass fraction and free CO_2 phase from the EPM method under scenarios with the EPP of 0.5 MPa, 0.50% salinity and different initial CO_2 mass fraction after 10 days. Distribution of **a** dissolved CO_2 mass fraction with 1.00% initial CO_2 mass fraction; **b** free CO_2 phase with 3.00% initial CO_2 mass fraction; **c** dissolved CO_2 mass fraction with 1.00% initial CO_2 mass fraction; **d** free CO_2 phase with 3.00% initial CO_2 mass fraction

For scenarios with 1.00% initial dissolved CO_2 mass fraction, the brine leakage rates from the EPM approaches are slightly smaller than that from T2Well for the scenarios where the EPP is less than 0.6 MPa (Fig. 15a). When the EPP is greater than 0.6 MPa, there is a divergence between the brine leakage rates from the two methods, which increases with the value of EPP. The brine leakage rates calculated by the EPM method for the scenarios of 1.0 and 1.5 MPa are much larger than the results of T2Well. The brine leakage rates are 26.9 and 34.5 kg/s at the EPP of 1.0 MPa using the T2Well and EPM methods, respectively. When EPP is 1.5 MPa, the brine flow rates become 34.2 and 52.5 kg/s for the T2Well and EPM methods, respectively.

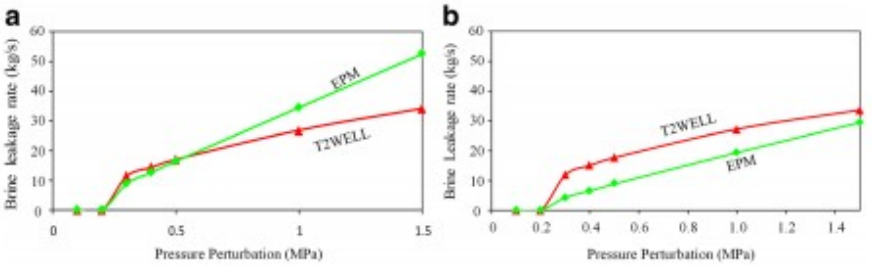

Fig. 15 Comparison of simulated brine leakage rates using the T2Well and EPM methods with different EPP and the same salinity (5.00%): **a** 1.00% dissolved CO_2 mass fraction; **b** 3.00% dissolved CO_2 mass fraction

For scenarios with 3.00% dissolved CO_2 mass fraction, it is much more obvious that the EPM method will under-estimate the brine leakage rates when the EPP exceeds 0.3 MPa, because of the self-limiting effect (Fig. 15b). It can be speculated that the brine leakage rates based on the EPM method will be beyond that from T2Well when the EPP becomes larger, such as 2.0 MPa. What is more, the results from the EPM method may be very sensitive to the equivalent permeability; thus, the EPM approach may under- or over-estimate the leakage rates for most of the scenarios, and it will become invalid when a large CO_2 phase appears because the physical model of the EPM approach is not suitable to handle flow in the wellbore.

The flux or the velocity of the flow through porous media can be simply determined from the gradient of pressure and gravity using Darcy's Law, and the conservation equation of mass components and energy can be generalized according to mass and energy conservation principles. While for fluid in the wellbore, besides the mass and energy conservation principles, the momentum conservation principle is necessary when determining the flow velocity. Taking the two-fluid condition as an example, Darcy's Law could not properly describe the flow dynamic in the wellbore because the wall friction is no longer the dominant resistance, but rather the interfacial force included in the drift-flux model is. The basic idea of drift-flux models is to assume that the gas velocity can be related to the volumetric flux of the mixture (gas phase and brine in this study) and the drift velocity of the gas, which is related to parameters like the gas saturation, wall friction factor, wellbore diameter, and so on. All of these ideas are transformed to the momentum equations by using the draft-flux model. Fundamentally, the T2Well/ECO2N simulator is more appropriate in handling problems like CO_2-brine leakage or CO_2 injection along the wellbore because the model is physically reasonable, while the EPM method is just an 'equivalent' method without considering the complicated flow in the wellbore.

Conclusions

The geological storage of CO_2 in saline aquifers has been recognized as one of the most significant potential ways to reduce CO_2 in the environment. For the safety of drinking-quality groundwater sources and a healthy ecology, the potential risk of CO_2 and brine leakage into shallow aquifers induced by CO_2 injection must be fully evaluated. This paper used a coupled wellbore-

reservoir model (T2Well/ECO2N) in water-CO_2-brine systems to analyze CO_2 and brine leakage through open wells. The hypothetical simulation model is comprised of a vertical wellbore surrounded by an idealized layered sequence of formations, with, from top to bottom, a shallow fresh aquifer, a shale formation with low permeability, and a deep saline aquifer. Parametric studies, including different values of salinity, EPP and the initially dissolved CO_2 mass fraction, were conducted to understand the leakage rate and the transition of different CO_2 phases. The findings are as follows:

1. EPP will push the brine and CO_2 upward along the open well. For the low EPP scenarios, there may be no CO_2 leakage into the fresh aquifer after 10 days. When EPP is increased greatly, the brine flow rate to the shallow aquifer will increase rapidly, and the brine leakage rates after 10 days increase almost proportionally with the EPP. The results also show that the brine leakage rate into the shallow aquifer will increase inversely with salinity.

2. The dissolved CO_2 mass fraction shows an important influence on the migration of the dissolved CO_2 plume after 10 days because part of the dissolved CO_2 becomes a free CO_2 phase. For the scenarios with a relatively low dissolved CO_2 mass fraction (0.10 and 0.50%), there is no phase transition of the dissolved CO_2; however, for the scenarios with a relatively high dissolved CO_2 mass fraction (1.00 and 3.00%), significant phase transition from the dissolved state to gas state occurs. As a result, the simulated dissolved CO_2 plume looks like a triangle for scenarios with a relatively low dissolved CO_2 mass fraction; however, the shape of the dissolved CO_2 plume becomes irregular for scenarios with a relatively high dissolved CO_2 mass fraction.

3. The effects of the CO_2 mass fraction on the brine leakage into the shallow aquifer are complicated and nonlinear depending on how significant the gas lifting effect is. For the cases of lower CO_2 mass fraction (e.g., 1.00% or below with other conditions investigated in this study), the CO_2 is expected to reduce the brine leakage rate slightly because the dissolution of CO_2 increases the density of the brine which effectively reduces the hydraulic gradient that is driving the brine flow. However, when the CO_2 mass fraction increases to a higher level (e.g., 3.00% or 3.89%) so that the gas phase occurs in the wellbore when the brine reaches a certain depth (below 700 m in the studied examples), the gas lifting effects will play a significant role and enhance the brine leakage in a degree proportional to the CO_2 mass fraction. Furthermore, the gas (CO_2-rich) phase leakage also becomes significant in addition to the brine leakage into the shallow aquifer in the case of the higher CO_2 mass fraction, which offers additional threat to the water quality of the shallow aquifer. The impact of the gas lifting effect caused by the gas phase and the self-limiting effect caused by salinity are opposite, while the results show that the self-limiting phenomenon still exists even if there appears to be a large amount of gas phase.

4. Comparative studies were performed to test the applicability of the equivalent porous media (EPM) approach to water-CO_2-brine systems. These studies found that the EPM approach may under- or over-estimate brine leakage rates under most scenarios for a fixed dissolved CO_2 mass fraction (1.0%). When the free CO_2 phase is evolved, there is a significant divergence of CO_2 and brine leakage between the EPM and T2Well results. The EPM approach will become invalid when a substantial free CO_2 phase appears because the momentum conservation is not involved in its physical model.

5. This study builds upon the first CO_2 capture and sequestration project in China, with a specific geothermal gradient and pressure gradient. Sensitivity analyses of three key factors that affect the CO_2-brine leakage—the EPP, salinity, and mass fraction of dissolved CO_2—were conducted to explore their effectiveness; however, factors like high heterogeneity and high geothermal and pressure gradients are also important, and are not fully discussed here.

Acknowledgements

We appreciate the constructive comments and suggestions from two anonymous reviewers.

Funding

This work was supported by the National Natural Science Foundation of China (Grant number: 41572220), the Fundamental Research Funds for the Central Universities (Grant Number: 2015KJJCB17), and the Research and Development Project on Geological Disposal of High-Level Radioactive Waste by the State Administration of Science, Technology and Industry for National Defense (Grant No. 2012-240).

References

Apps JA, Zheng L, Zhang Y, Xu T, Birkholzer JT (2010) Evaluation of potential changes in groundwater quality in response to CO_2 leakage from deep geologic storage. Transport Porous Med 82:215–246. https://doi.org/10.1007/s11242-009-9509-8

Bachu S (2000) Sequestration of CO_2 in geological media: criteria and approach for site selection in response to climate change. Energ Convers Manage 41:953–970. https://doi.org/10.1016/S0196-8904(99)00149-1

Bigi S, Battaglia M, Alemanni A, Lombardi S, Campana A, Borisova E, Loizzo M (2013) CO_2 flow through a fractured rock volume: insights from field data, 3D fractures representation and fluid flow modeling. Int J Greenh Gas Con 18:183–199

Birkholzer JT, Nicot JP, Oldenburg CM, Zhou Q, Kraemer S, Bandilla K (2011) Brine flow up a well caused by pressure perturbation from geologic carbon sequestration: static and dynamic evaluations. Int J Greenh Gas Con 5(4):850–861

Birkholzer JT, Zhou Q, Tsang C (2009) Large-scale impact of CO_2 storage in deep saline aquifers: a sensitivity study on pressure response in stratified systems. Int J Greenh Gas Con 3:181–194

Duan Z, Sun R (2003) An improved model calculating CO_2 solubility in pure water and aqueous NaCl solutions from 273 to 533 K and from 0 to 2000 bar. Chem Geol 193(3–4):257–271

Duan Z, Sun R, Zhu C, Chou IM (2006) An improved model for the calculation of CO_2 solubility in aqueous solutions containing Na^+, K^+, Ca^{2+}, Mg^{2+}, Cl^-, and SO_4^{2-}. Mar Chem 98(2–4):131–139

Esposito A, Benson SM (2012) Evaluation and development of options for remediation of CO_2 leakage into groundwater aquifers from geologic carbon storage. Int J Greenh Gas Con 7:62–73

Ford EP, Moeinikia F, Lohne HP, Øystein, Majoumerd MM, Fjelde KK (2017) Leakage calculator for plugged and abandoned wells. SPE Bergen one day seminar, Bergan, Norway, 5 April 2017

Harp DR, Pawar R, Carey JW, Gable CW (2016) Reduced order models of transient CO_2 and brine leakage along abandoned wellbores from geologic carbon sequestration reservoirs. Int J Greenh Gas Con 45:150–162

Hu L, Chen C, Chen X (2011) Simulation of groundwater flow within observation boreholes for confined aquifers. J Hydrol 398:101–108

Hu L, Pan L, Zhang K (2012) Modeling brine leakage to shallow aquifer through an open wellbore using T2Well/ECO2N. Int J Greenh Gas Con 9:393–401

Huerta NJ, Vasylkivska VS (2015) Well leakage analysis tool (WLAT) user's manual. National Energy Technology Laboratory, Morgantown, WV

Humez P, Audigane P, Lions J, Chiaberge C, Bellenfant G (2011) Modeling of CO_2 leakage up through an abandoned well from deep saline aquifer to shallow fresh groundwaters. Transport Porous Med 90:153–181. https://doi.org/10.1007/s11242-011-9801-2

Jung Y, Zhou Q, Birkholzer JT (2013) Early detection of brine and CO_2 leakage through abandoned wells using pressure and surface-deformation monitoring data: concept and demonstration. Adv Water Resour 62:555–569

Liu H, Hou Z, Were P, Gou Y, Xiong L, Sun X (2015) Modelling CO_2-brine-rock interactions in the upper Paleozoic formations of Ordos Basin used for CO2 sequestration. Environ Earth Sci 73:2205–2222. https://doi.org/10.1007/s12665-014-3571-4

Mualem Y (1976) A new model for predicting hydraulic conductivity of unsaturated porous-media. Water Resour Res 12:513–522. https://doi.org/10.1029/WR012i003p00513

Namhata A, Zhang L, Dilmore RM, Oladyshkin S, Nakles DV (2017) Modeling changes in pressure due to migration of fluids into the above zone monitoring interval of a geologic carbon storage site. Int J Greenh Gas Con 56:30–42

Nordbotten JM, Celia MA, Bachu S (2004) Analytical solutions for leakage rates through abandoned wells. Water Resour Res 40:1035–1042. https://doi.org/10.1029/2003WR002997

Nordbotten JM, Celia MA, Bachu S, Dahle HK (2005) Semianalytical solution for CO_2 leakage through an abandoned well. Environ Sci Technol 39:602–611. https://doi.org/10.1021/es035338i

Nordbotten JM, Kavetski D, Celia MA, Bachu S (2009) Model for CO_2 leakage including multiple geological layers and multiple leaky wells. Environ Sci Technol 43:743–749. https://doi.org/10.1021/es801135v

Pan LH, Oldenburg CM (2014) T2Well-an integrated wellbore-reservoir simulator. Comput Geosci-UK 65:46–55

Pan LH, Oldenburg CM, Pruess K, Wu YS (2011a) Transient CO_2 leakage and injection in wellbore-reservoir systems for geologic carbon sequestration. Greenh Gas Sci Technol 1:335–350. https://doi.org/10.1002/ghg

Pan LH, Oldenburg CM, Wu Y, Pruess K (2011b) T2Well/ECO2N version 1.0: multiphase and non-isothermal model for coupled wellbore-reservoir flow of carbon dioxide and variable salinity water. Report no. LBNL-4291E, Lawrence Berkeley Natl. Lab., Berkeley, CA

Pan LH, Webb SW, Oldenburg CM (2011c) Analytical solution for two-phase flow in a wellbore using the drift-flux model. Adv Water Resour 34(12):1656–1665

Pawar RJ, Watson TL, Gable C (2009) Numerical simulation of CO_2 leakage through abandoned wells: model for an abandoned site with observed gas migration in Alberta, Canada. Energy Procedia 1(1):3625–3632. https://doi.org/10.1016/j.egypro.2009.02.158

Réveillère A (2013) Semi-analytical solution for brine leakage through passive abandoned wells taking account of brine density differences. Transport Porous Med 100:337–361. https://doi.org/10.1007/s11242-013-0221-3

Steel L, Liu Q, Mackay E, Maroto-Valer MM (2016) CO_2 solubility measurements in brine under reservoir conditions: a comparison of experimental and geochemical modeling methods. Greenhouse Gas Sci Technol 6(2):197–217

Tao Q, Checkai D, Huerta N, Bryant SL (2011) An improved model to forecast CO_2 leakage rates along a wellbore. Energy Procedia 4:5385–5391. https://doi.org/10.1016/j.egypro.2011.02.522

Tao Q, Checkai D, Huerta N, Bryant SL (2014) Estimating CO_2 fluxes along leaky wellbores. SPE J 19:227–238. https://doi.org/10.2118/135483-PA

Tao Q, Bryant SL (2014) Well permeability estimation and CO_2 leakage rates. Int J Greenh Gas Con 22:77–87

Van Genuchten MT (1980) A closed-form equation for predicting the hydraulic conductivity of unsaturated soils. Soil Sci Soc Am J 44(5):892–898

Xie J, Zhang K, Hu L, Wang Y, Chen M (2015) Understanding the carbon dioxide sequestration in low-permeability saline aquifers in the Ordos Basin with numerical simulations. Greenhouse Gas Sci Technol 5(5):558–576

Yamamoto H, Zhang K, Karasaki K, Marui A, Uehara H, Nishikawa N (2009) Large-scale numerical simulation of CO_2 geologic storage and its impact on regional groundwater flow: a hypothetical case study at Tokyo Bay, Japan. Energy Procedia 1(1):1871–1878

Yu B, Wang L, Liu Y (2016) Optimization of injection location based on simulations of CO_2 leakage through multiple leakage pathways. Asia Pac J Chem Eng 11:620–629. https://doi.org/10.1002/apj.1990

Zhang K, Xie J, Li C, Hu L, Wu X, Wang Y (2016) A full chain CCS demonstration project in northeast Ordos Basin, China: operational experience and challenges. Int J Greenh Gas Con 50:218–230

Zhang M, Bachu S (2011) Review of integrity of existing wells in relation to CO_2 geological storage: what do we know? Int J Greenh Gas Con Control 5(4):826–840

Zheng L, Apps JA, Zhang Y, Xu T, Birkholzer JT (2009) On mobilization of lead and arsenic in groundwater in response to CO_2 leakage from deep geological storage. Chem Geol 268(3–4):281–297

Zhu C, Zhang G, Lu P, Meng L, Ji X (2015) Benchmark modeling of the Sleipner CO_2 plume: calibration to seismic data for the uppermost layer and model sensitivity analysis. Int J Greenh Gas Con Control 43:233–246